



DEVELOPMENT OF A LOW-COMPLEXITY OUTPATIENT CARDIAC HEALTH ASSESSMENT SYSTEM FOR IoMT NETWORKS

¹V. Simhadri, ²P. Poojitha, ³K. Sireesha Sai Priya, ⁴P. Uma Maheswari, ⁵K. Veerashish

Dept of ECE, Godavari Institute of Engineering and Technology(A), Rajahmundry

^{2,3,4,5}Students, Dept of ECE, Godavari Institute of Engineering and Technology (A), Rajahmundry

Abstract-Heartdiseases and stroke have both contributed significantly to the rising death rates across all age categories in recent decades. As a result of lifestyle changes and dietary preferences, this has occurred. If you want to keep your heart in tip-top shape, it is crucial to have your heart checked often. Because of this, the mortality rate may be lowered when therapy is given quickly and efficiently. The health and efficiency of the circulatory system may be determined by a comprehensive examination of the heart Our goal in this article is to create a simple cardiac evaluation system using the IoMT in the medical field. Interoperability in Medical Terminology (IoMT) addresses medical terminology and provides trustworthy analysis that is both low-cost and easy to integrate with other systems. These IoMT services are available to patients. As a result, the patient's quality of life would rise. Since IoMT can save time and accomplish more, it has gained in popularity. The healthcare sector has seen a dramatic transformation due to IoMT. With this IoMT, we may anticipate not only an accurate result but also a quicker one. We have observed results for many online databases. Proposed algorithm shows the overall the accuracy is 98.4%, sensitivity is 99% and positive predictivity is 97.1% for detecting systolic peaks. Further Proposed algorithm shows the overall the accuracy is 98.8%, sensitivity is 100% and positive predictivity is 97.9% for detecting peak onsets. And real recorded data has 98.2% of accuracy.

Keywords: *IoMT, HEART DISEASE, ECG, PPG*

1. INTRODUCTION

Some health studies report that heart attacks are the cause of death for 14% of all persons each year. Detecting cardiovascular illnesses is challenging because of their subtle symptoms. To better understand how the cardiovascular system works, it is important to do a thorough inspection and evaluation of the heart. Smart gadgets and technological advancements have brought about notable change in the medical health care sector's approach to addressing health problems. Mobile Internet of Things devices may connect users to a variety of healthcare options. Future of Healthcare will be provided by the IoMT (Internet of Medical Things). The IoMT will revolutionise the medical industry in the future. Because of its potential for increased efficiency and time savings, IoMT has gained in popularity. This is a game-changing shift in the medical industry. High precision is to be expected with the time savings when utilising IoMT. Using sophisticated sensors, we can capture the heart's electrical impulses. This is an easy and fast way to evaluate the data in a brief time. Typically, IoT sensors are placed on people to record their vital signs and track other health metrics in real time. Predicting risk early allows for more effective treatment, and data collection, processing, and analysis are all key steps.

1.1 ECG:

The electrocardiogram is a test that captures the heart's electrical activity to diagnose several cardiac problems. Electrodes implanted on the chest induce a heartbeat, allowing for the recording of electrical impulses. The

waves representing the signals are shown on a screen. A sinus node generates the electrical impulse at a rate of 60-90 beats per minute. It is also referred to as an electrocardiogram. In a person who does not exhibit any of the risk factors for heart disease (such as high blood pressure) or the symptoms of heart disease, the test is meaningless (such as chest discomfort). However, ECGs are often performed as part of regular checks, and many patients who have neither risk factors nor symptoms get them.

ABNORMALITIES OF ECG:

Several potential health issues may be reflected by an irregular electrocardiogram. However, certain irregularities on an electrocardiogram are perfectly typical variations in cardiac rhythm. Other folks may need daily medicine intake to maintain a more regular heart rate. It may be essential to perform cardiac catheterization or surgery on a person having a heart attack to restore blood flow to the heart. If the PR interval is more than 0.2s, we call it a block in the first degree of the AV node. The wait between the p wave and the QRS complex will be longer, but the other waves will be there.

1.2 PPG:

An optically acquired plethysmogram or photo plethysmogram may be used to measure microvascular blood volume fluctuations. PPG is a simple and inexpensive optical method for monitoring microvascular blood volume changes. Signal from the photoplethysmography (PPG) and associated electrocardiogram with pulsatile component.

It is often used for non-invasive measurement at the skin's surface. Heartbeat-induced fluctuations in blood volume cause the pulsating physiological waveform (termed as "AC" waveform) that makes up the PPG. Lower frequency components of this waveform are associated with respiration, sympathetic nervous system activity, and thermoregulation, and they are superimposed over a slowly fluctuating (referred to as a "DC") baseline. It is accepted that the PPG signal may provide valuable insights into the cardiovascular system, yet its components' origins remain unclear. Differentiating irregularities in PPG signals may be accomplished by calculating the distance between character sequences using both local and global data. When the separation is more than a certain value, it is seen as an abnormal pattern. The proposed method may be used to analyze a wide variety of physiological data.

2. PROPOSED ALGORITHM

In this section we are using the algorithm to detect the systolic peaks in ECG/PPG. This includes the steps

- Bandpass Filtering and Differentiation
- New Nonlinear Transformation
- New Peak-Finding Technique
- Finding Location of True R-Peaks

Differentiation and Bandpass Filtering

Many artifacts and disturbances from the outside world sometimes obscure ECG signals in real-world settings. Common causes of ECG noise include power line interference, muscular contractions, baseline drift from breathing, and rapid baseline change. The fundamental frequencies of a QRS complex are about 530 hertz. P/T waves and motion artifacts concentrate the majority of their noise energy up to 5 Hz. There must be enough protection against P/T waves and noise up to 5 Hz. A spectral analysis of QRS geometries ranging in length from 0.05 to 0.2 s reveals that the majority of the frequencies included in the QRS complex are below 20 Hz. To maximise the energy of different QRS complexes while minimising the effects of P/T waves, powerline interference, motion artifacts, and muscle noise, the passband was chosen for this research (narrow-QRS and wide-QRS complexes).

To create a passband with cutoff frequencies of 6 and 20 Hz, we use the least squares approach to construct a 15th-order FIR bandpass DF. To emphasise the high-frequency and large-slope information included in the QRS complex, we use first-order forward differentiation after filtering. Here, we see $f[n]$ differentiated in the form as:

$$d[n] = f[n+1] - f[n]$$

New Nonlinear Transformation

Squaring and Adaptive Thresholding

An adaptive threshold is applied to the energy (or squarer) values of $e[n]$, after the dECG signal $d[n]$ has been squared to make it positive-valued. The squaring is accomplished by first converting the negative dECG signal $d[n]$ to a positive one (through squaring), and then applying adaptive thresholding on the resulting positive $e[n]$ energy values. Specifically, the squaring occurs as

$$e[n] = d^2[n]$$

The thresholding function is defined as

$$E_{th}[n] = \begin{cases} 0, & e[n] < g \\ e[n], & otherwise \end{cases}$$

In this thresholding technique, the energy values $e[n]$ that are less than the threshold parameter g are set to zero. Adaptive threshold parameter g is determined for each ECG segment.

$$g = 0.5 * \sigma_e,$$

$$\text{where } \sigma_e = \sqrt{\frac{1}{M} \sum_{m=1}^M (e[n] - \alpha)^2} \text{ and } \alpha = \frac{1}{M} \sum_{m=1}^M e[n]$$

Shannon Energy Computation and Smoothing

A finite-impulse response (FIR) filter with a rectangular impulse response $h[k]$ of length L is used to smooth the Shannon energy values, reducing the effect of several peaks in the QRS complex. This smoothing process is meant to result in peaks that correspond to the QRS-complex sub-sections. The sleek characteristic signal that the proposed nonlinear transformation generated. Approximate placements of the R peaks in the given ECG waveform agree with the locations of the candidate R-peaks in the SE envelope $s[n]$. Our proposed method analyses these candidate peaks further in order to identify the true R peaks in an ECG signal. The change in Shannon energy causes a little shift in the position of the R peak between iterations. We have already studied the efficacy of this nonlinear transformation. Based on experimental findings, it improves detection in both tiny and big QRS complex ECG signals. Then, the signal's threshold energy must be normalized as

$$\overline{e_{th}}[n] = \frac{e_{th}[n]}{\max_{m=1}^M (e_{th}[n])}$$

And Shannon energy of the normalized signal $\overline{e_{th}}[n]$ is computed as

$$s[n] = -e_{th}^{-2}[n] \log e_{th}^{-2}[n]$$

Smoothing the Shannon energy values using a finite-impulse response (FIR) filter with a rectangular impulse response $h[k]$ of length L reduces the impact of several peaks in the vicinity of QRS complex regions. These peaks should line up with the QRS-complex components, which is why a smoothing process is used. When applied, the suggested nonlinear transformation results in a clean feature signal. It is easy to see that the estimated positions of R peaks in the ECG waveform correspond roughly to the locations of potential R-peaks in the SE envelope $s[n]$. So, our proposed method involves processing these candidate peaks to identify true R peaks in an ECG signal.

New Peak-Finding Technique

In this subsection, we provide an innovative and straightforward peak-finding approach that leverages the first-order Gaussian differentiator (FOGD)

operator to quickly and easily locate probable R-peaks in the SE envelope. A Differentiator of Gaussian Functions of the First Order

Here N point Gaussian window $w[n]$ is defined as

$$w[n] = e^{-\frac{1}{2} \left[\frac{n - \frac{N}{2}}{\rho} \right]^2} \text{ where, } n = 1, 2, 3, \dots, N$$

And FOGD is written as

$$w_d[n] = w[n+1] - w[n], \text{ where } n=1, 2, 3, \dots, N-1$$

The slope at each sample is depicted as the 901-point Gaussian window with spread $r = 36$, and the associated FOGD function.

The Gaussian window is symmetric at $[N/2] + 1$ and its first order derivative is an asymmetric function. And the Gaussian window function is having peak at $n = [N/2] + 1$. Thus, the slope of FOGD is positive and negative for $1 \leq n \leq \frac{N}{2}$ and $\frac{N}{2} + 1 \leq n \leq N$, and it is zero at $n = \frac{N}{2}$. The proposed peak-finding logic is based on this. We perform a convolution operation on the SE envelope $s[n]$ and the FOGD sequence $w_d[m]$ to identify potential R-peaks in the SE envelope. And FOGD sequence is computed as

$$Z[n] = \sum_{l=-\infty}^{\infty} w_d[l] s[n-l]$$

FOGD function $w_d[m]$ output convolved with a Shannon energy envelope $s[n]$. Since the FOGD function is anti-symmetric, we refer to the convolution output (both positive and negative ZCs) as the ZC function ($z[n]$) in this paper. When the signal flips from negative to positive, you may get a ZC that has a positive slope and is thus positive. The transition from positive to negative signal $z[n]$ represents a negative ZC with a negative slope. As can be seen in Figure 5c, the maxima of the Shannon energy envelope $s[n]$ are located at negative ZCs. The development and use of negative ZCs follows.

Detecting Negative Zero-crossings

In this research, negative ZCs were identified by comparing the signs of the ZC function $z[n]$ at time instants t_n and t_{n+1} . Potential R-peaks in the SE envelope are located at the right times using the proposed peak-finding method. The times of detection are not precisely in sync with the times of the authentic R peaks in the ECG signal. That's why we use the timestamps at which potential R-peaks have been recognized as landmarks for locating the real deal.

Finding Location of True R-Peaks

Time instants of real R-peaks in an original ECG signal are determined by using the positions of all candidate

R-peaks obtained in the prior step. To begin, the region of the original ECG signal including each possible R-peak is reconstructed. After that, the biggest peak value in the section is found using a simple technique. This procedure is repeated for each location $p[m]$ that has been uncovered. The results show that accurate R-peak localizations may be determined even when dealing with noise and irregularly shaped QRS complexes.

Algorithm Implementation and Assessment

The proposed method is realised in MATLAB on an Intel Core 2 Quad processor running at 2.4 GHz. The technique is tested on data from the MIT-BIH arrhythmia database and the slpdb [18-19] database (<https://archive.physionet.org/physiobank/database/slpdb/>). In the ECG signal, the larger value of M may join two adjacent R-peaks. In this analysis, the smoothing filter length is determined by averaging the minimum and maximum values for the QRS complex. The usual duration of a normal or wide QRS complex is 0.05 to 0.2 seconds. The duration of the filtering process is calculated using a sampling rate of 360 times per second. Here, we take into account a few measures, such as the sensitivity [Se], accuracy [Acc], predictivity [+P], and detection error rate [DER]. The Se is the fraction of the original ECG signal's R-peaks that were successfully recognised by the algorithm. When comparing the overall number of peaks detected by the algorithm to the number of true R-peaks, the +P is the ratio of the two. Calculating Parametric Elements:

$$Se = TP / (TP + FN) * 100 \%$$

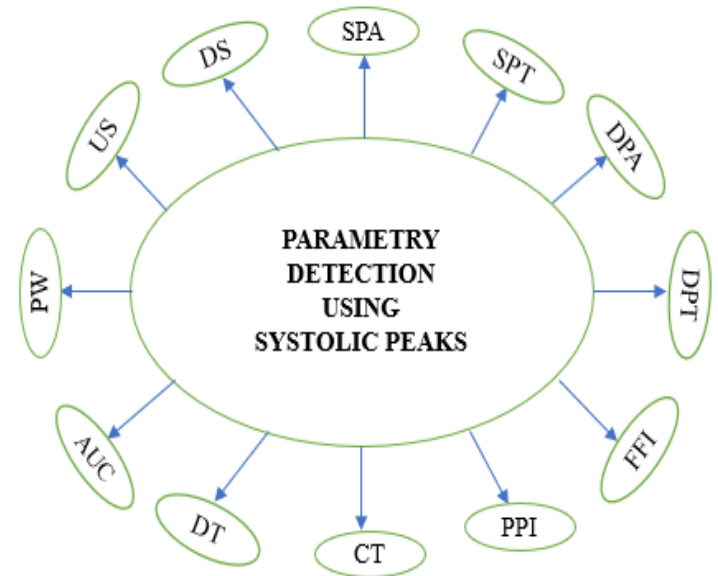
$$Acc = TP / (TP + FP + FN) * 100 \%$$

$$P = TP / (TP + FP) * 100 \%$$

$$DER = (FP + FN) / TP * 100 \%$$

Parametry Detection

There are some parameters which are required to detect after peak detection. They are:



SPA – Systolic Peak Amplitude

SPT – Systolic Peak Time

DPA – Diastolic Peak Amplitude

DPT – Diastolic Peak Time

FFI – Foot to Foot Interval

PPI – Peak to Peak Interval

CT – Crest Time

DT – Decay Time

AUC – Area Under Curve

PW – Pulse Width

US – Upslope

DS – Downslope

3. METHODOLOGY:

PPG Analysis:



Fig3.1: Block Diagram

Signal Acquisition: Data is acquired from existing databases or obtained from the Proto central MAX86150 device for ECG and PPG signals. The required MATLAB file is generated by recording and transforming ECG and PPG data. Files of this kind may be imported into Matlab and processed.

Filtering: There is background noise in the data. Filtering these signals is required for noise suppression. To achieve filtering, the median filter is used here. Filtering is applied depending on the characteristics of the input signal. The median filter is used to find a signal's midpoint.

Signal Quality Testing: The signal is being tested right now. When filtering is done, the signal is checked for quality. For any differences, we make the necessary adjustments to the signal. A revised plan is implemented in the next phase.

Peak Detection: After checking for quality is finished, peak detection comes next. There is a focus on the peaks of the ECG and PPG waveforms. Using peak detection, malfunctioning signals may be isolated.

Parametry Detection: We do signal analysis to get the values for the various parameters and plug them into our equations. Some examples of such metrics are the systolic and diastolic times of peak, the times between peaks, the times at the crest and the times of decline and the area under the curve. Any of these may be used to assess the health and function of the heart.

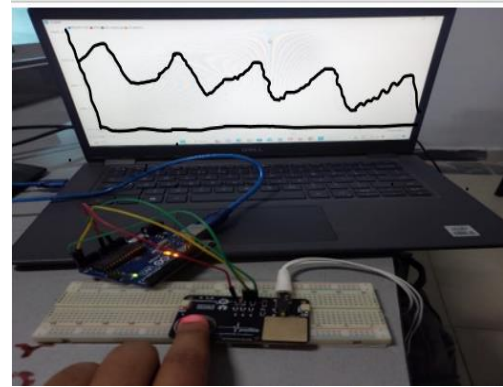


Fig3.2: Figure shows the recording of the real PPG signal

The pins of the Arduino Uno is connected to Protocentral MAX86150 in the following way.

MAX86150	Arduino Uno
VCC	5 V
GND	GND
SDA	A4
SCL	A5

Now the fingertip is placed on the sensor and observe the PPG waveforms on the Arduino platform. Record the values and converted them to matlab file for peak detection and also for Parametry detection.

ECG Analysis:

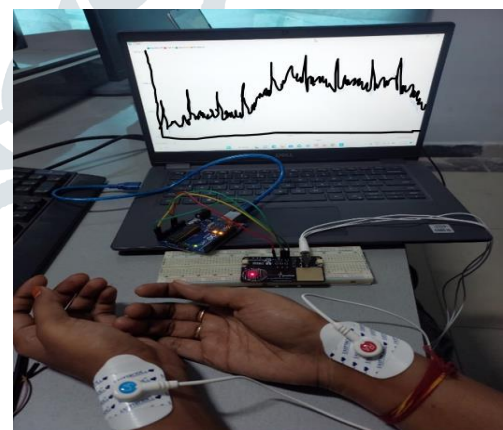


Fig3.3: Figure shows the recording of the real ECG signals connection of left arm node is given to left hand, right arm node to the right arm and right leg node to the right leg.

IMPLEMENTATION:

PERFORMANCE OF THE PROPOSED ALGORITHM FOR SYSTOLIC PEAKS

Record	TSP	FP	FN	Se	Acc	Pp	DER
slp01am	3854	10	1	99.9	99.7	99.7	0.002
slp02am	6143	4	0	100	99.9	99.9	0.0006
slp02bm	5442	8	0	100	99.8	99.8	0.001
slp04m	5448	12	0	100	99.7	99.7	0.002
slp14m	4330	9	0	100	99.7	99.7	0.002
slp16m	5623	2	0	100	99.6	99.6	0.0003
slp32m	4562	6	0	100	99.8	99.8	0.0013
slp37m	5670	2	0	100	99.9	99.9	0.0003
slp41m	5009	1	0	100	83.6	83.6	0.0001
slp48m	4722	5	0	100	99.8	99.8	0.001
slp59m	5121	0	0	100	100	100	0
slp60m	4902	3	0	100	99.9	99.9	0.0006
slp61m	4998	5	1	99.9	99.8	99.9	0.001
slp66m	5459	3	0	100	99.9	99.9	0.0005
slp67xm	4732	1	0	100	99.9	99.9	0.0002
slp03m	4501	0	0	100	100	100	0
slp45m	3854	10	1	99.9	99.7	99.7	0.002

TSP= Total systolic peaks

FP=False positive

FN=False negative

Se= Sensitivity

Acc= Accuracy

Pp= Positive Predictivity

DER= Detection error rate

PERFORMANCE OF THE PROPOSED ALGORITHM FOR DIASTOLIC PEAKS							
Record	TDP	FP	FN	Se	Acc	Pp	DER
slp01am	3803	1	0	100	99.9	99.9	0.0002
slp02am	6071	9	0	100	99.8	99.8	0.001
slp02bm	5347	36	0	100	99.3	99.3	0.006
slp04m	5795	5	0	100	99.9	99.9	0.0008
slp14m	4221	51	0	100	98.8	98.8	0.012
slp16m	5649	5	0	100	99.9	99.9	0.0008
slp32m	4498	162	0	100	96.5	96.5	0.036
slp37m	5631	2	0	100	99.9	99.9	0.0003
slp41m	4572	57	0	100	98.7	98.7	0.012
slp48m	4570	10	0	100	99.7	99.7	0.002
slp59m	4992	4	0	100	99.9	99.9	0.0008
slp60m	4893	3	0	100	99.9	99.9	0.006
slp61m	4966	2	0	100	99.9	99.9	0.0004
slp66m	4558	4	0	100	99.9	99.9	0.008
slp67xm	4592	3	0	100	99.9	99.9	0.0006
slp03m	4427	4	0	100	99.9	99.9	0.0009
slp45m	5056	6	0	100	99.8	99.8	0.001

TDP = Total diastolic peaks

$$Se = TP / (TP + FN) * 100 \%$$

$$Acc = TP / (TP + FP + FN) * 100\%$$

$$Pp = TP / (TP + FP) * 100\%$$

$$DER = (FP + FN) / TP * 100\%$$

4. RESULTS

4.1 ECG Result Analysis:

The proposed work is tested and analyzed with different databases and real timesignals. The parameters include systolic peak amplitude, systolic peak time and peak to peak interval. Here, for the slp01am signal, the accuracy is 99.9%, sensitivity is 100% and positive predictivity is 99.99%.

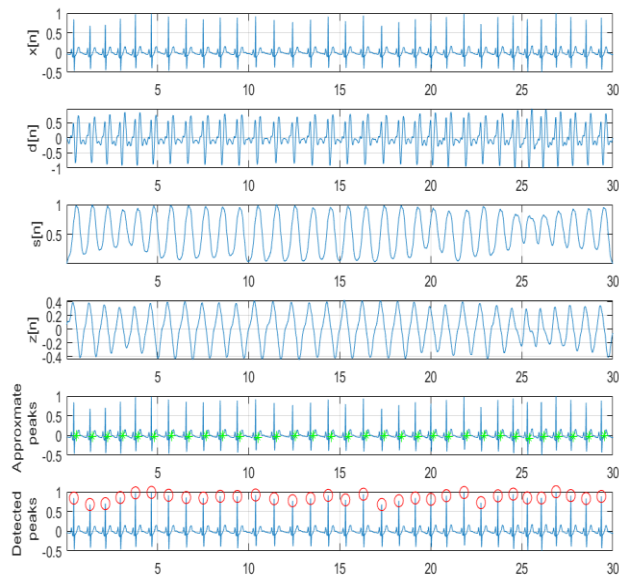


Fig4.1.1: Peak detection of the ECG signal using proposed algorithm for the systolic peaks in 30 secs of time

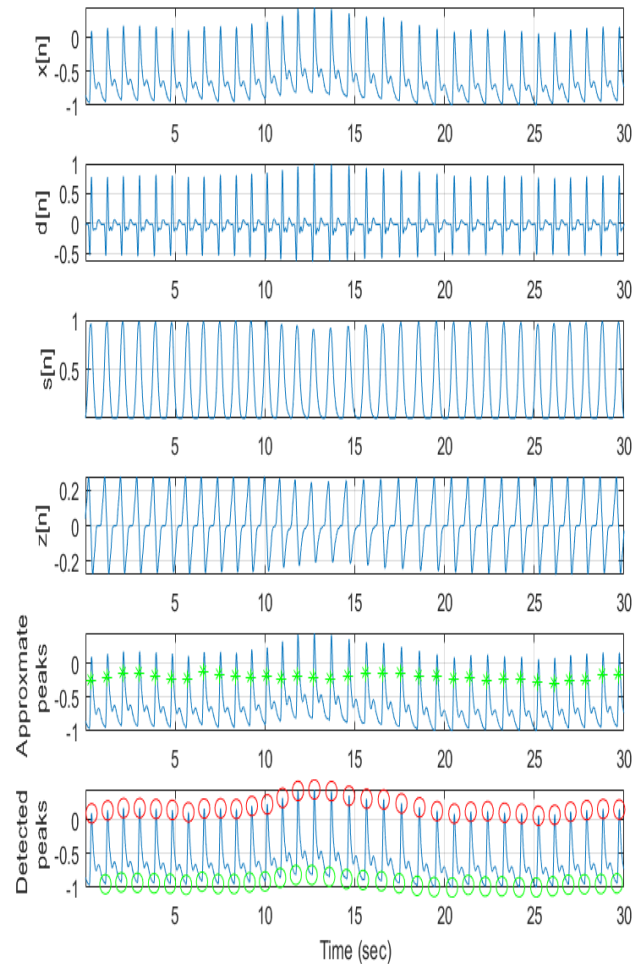


Fig4.2.1: Peak detection of the PPG signal using proposed algorithm for the systolic peaks in 30 secs of time. Here $x[n]$ is original signal, $d[n]$ is difference of filtered signal, $s[n]$ is Shannon Energy, $z[n]$ is Gaussian Energy.

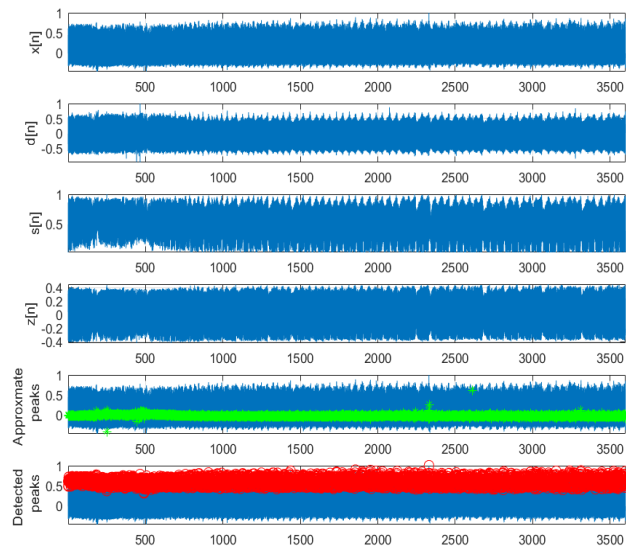


Fig4.1.2: Peak detection of the ECG signal using proposed algorithm for the systolic peaks in 36000 secs of time

4.2 PPG Result Analysis:

The parameters include systolic peak amplitude, systolic peak time, diastolic peak amplitude, diastolic peak time peak to peak interval, foot to foot interval, crest time, decay time, area under curve upslope and downslope. Here, for the slp02am signal, the accuracy is 99.8%, sensitivity is 100% and positive predictivity is 99.8%.

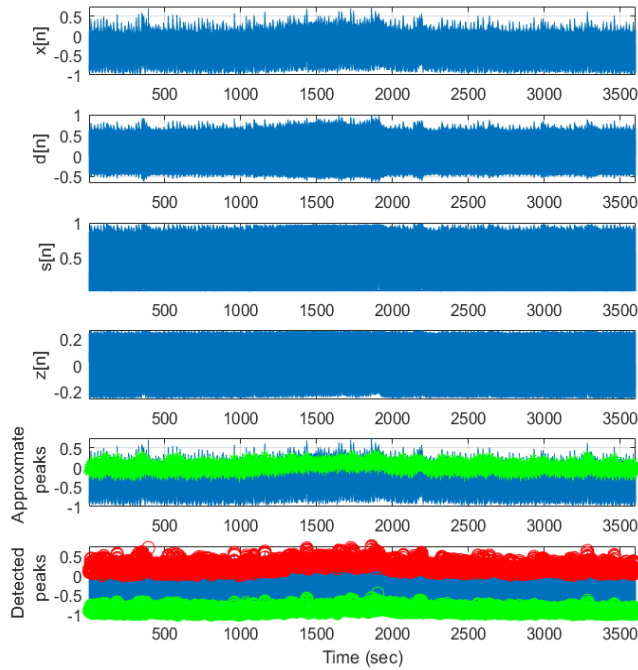


Fig4.2.2: Peak detection of the PPG signal using proposed algorithm for the systolic and d peaks in 3600 secs of time

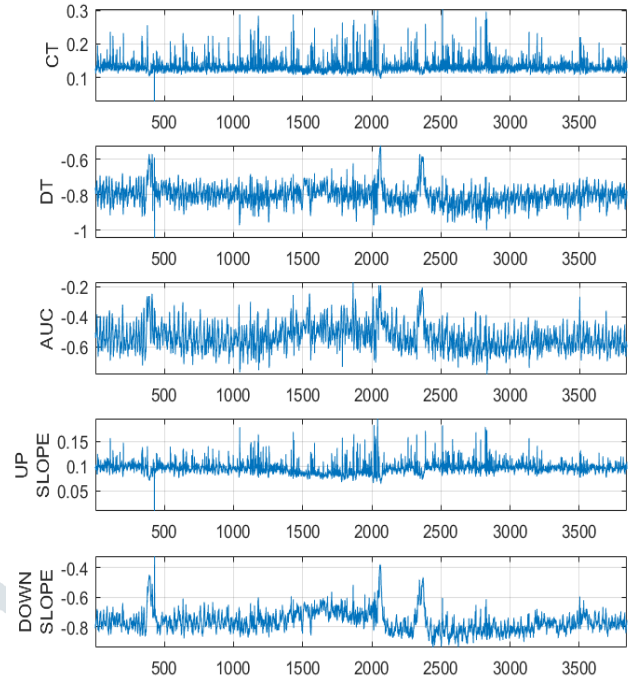


Fig4.2.4: Parametry detection of the PPG signal using proposed algorithm

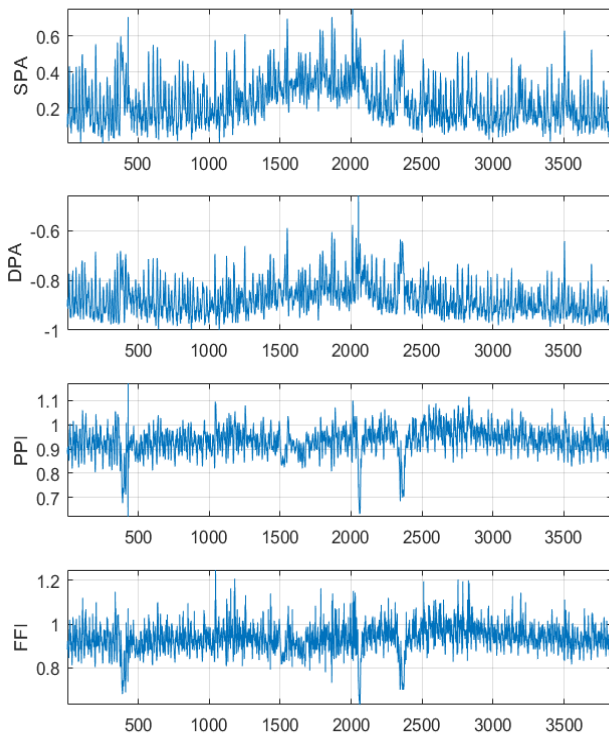


Fig4.2.3: Parametry detection of the PPG signal using proposed algorithm

5. CONCLUSION

In this study, we suggested a novel systolic peak and onset detection for the automatic processing of PPG data. An easy-to-implement technique is presented in this work for automated R-peak detection in an electrocardiogram. This approach incorporates novel transformations and straightforward peak-finding methods. Our results are quite precise; we've managed to drastically cut down on both false positives and negatives. Noise signals are attenuated, then peak detection is performed on the positives. The suggested system analyses a wide variety of signals, both those stored in a database and those occurring in real time. A total of 60 minutes are spent analyzing the various signals. The accuracy rate varies depending on the signal. Proposed algorithm shows the overall the accuracy is 98.4%, sensitivity is 99% and positive predictivity is 97.1% for detecting systolic peaks. Further Proposed algorithm shows the overall the accuracy is 98.8%, sensitivity is 100% and positive predictivity is 97.9% for detecting peak onsets. And real recorded data has 98.2% of accuracy.

REFERENCES

- ¹Made F, Nonterah EA, Tlotleng N, Ntlebi V, Naicker N. Ten-year risk of fatal cardiovascular disease and its association with metabolic risk factors among waste pickers in South.
- ²R.N.Patel and M. P. Barot, "Development Of Methodology for Precise Diagnosis MoMoody GB, Mark RG, "The impact of the MIT-BIH arrhythmia database," IEEE Engineering in Medicine and Biology Magazine, vol. 20, no. 3, pp.45-50, May/June 2001.
- ³Moody GB, Mark RG, "The impact of the MIT-BIH arrhythmia database," IEEE Engineering in Medicine and Biology Magazine, vol. 20, no. 3, pp.45-50, May/June 2001.
- ⁴H. Khattak, M. Ruta, and P. di Bari, "CoAP-based Healthcare Sensor Networks: a survey," in Proceedings of the 11th International Bhurban Conference on Applied Sciences and Technology, 2014.
- ⁵J. Padikkapparambil, C. Ncube, K. K. Singh, and A. Singh, "Internet of Things technologies for elderly health-care applications," Emergence of Pharmaceutical Industry Growth with Industrial IoT Approach, 2020.
- ⁶R. A. Ramlee, M. H. Leong, R. S. Sarban Singh, M. M. Ismail, M. A. Othman, H. A. Sulaiman, M. H. Misran, M. Said, M. Alice et al., "Bluetooth remote home automation system using android application", The International Journal of Engineering and Science (IJES), vol. 2, no. 1, pp. 149-153, 2013.
- ⁷A. Mohanty, I. Obaidat, F. Yilmaz, and M. Sridhar, "Control-hijacking vulnerabilities in IoT firmware: A brief survey," in The 1st International Workshop on Security and Privacy for the Internet-of-Things (IoTSec), 2018.
- ⁸Rim Negra, Imen Jemili, Abdelfettah Belghith, "Wireless Body Area Networks: Applications and technologies", Elsevier-2016, <https://cyberleninka.org/article/n/633432.pdf>, 23/4/2022.
- ⁹A. Mathew, S. Zhang, L. Ma, T. Earle, D. Hargreaves Reducing maintenance cost through effective prediction analysis and process integration, Proceedings of the VETOMAC-3 & ACSIM2004: 604-611, 2004.
- ¹⁰Corrado D, Basso C, Schiavon M, et al. Pre-participation screening of young competitive athletes for prevention of sudden cardiac death. J Am Coll Cardiol. 2008;52(24):1981–1989. doi:10.1016/j.jacc.2008.06.053.
- ¹¹Kompletecare. Kompletecare Benefit Package. <http://www.kompletecare.com>. Accessed 28 October 2020.
- ¹²Shahkar, S.; Shen, Y.; Khorasani, K. Diagnosis, prognosis and health monitoring of electrohydraulic servo valves (EHSV) using particle filters. In Proceedings of the 6th International Conference on Control, Decision and Information Technologies (CoDIT), Paris, France, 23–26 April 2019.
- ¹³Blum, J. (2013). Exploring Arduino: tools and techniques for engineering wizardry. John Wiley & Sons
- ¹⁴Yi, X.J. Health Estimation and Prognostics for Complex Electromechanical System Based on Semi-Quantitative Information. Master's Thesis, ChangChun University of Technology, Changchun, China, 2017.
- ¹⁵Anand, S. and Sharma, A. (2020). Assessment of security threats on IoT based applications. Materials.Today:Proceedings. doi: 10.1016/j.matpr.2020.09.350
- ¹⁶Yin, Y.; Zhang, M.; Wei, X.; Nie, H.; Chen, H. Fault analysis and solution of an airplane nose landing gear's emergency lowering. J. Aircr. 2016, 53, 1022–1032. [CrossRef]
- ¹⁷TLV. Tandvårds-Läkemedelförmånsverket. [cited 2019 Jun 08] Organisation -Available from: <https://www.tlv.se/in-english/organisation.html>
- ¹⁸<https://archive.physionet.org/physiobank/database/slpdb/>
- ¹⁹<https://archive.physionet.org/physiobank/database/mitdb/>